Fibers and Polymers
https://doi.org/10.1007/s12221-024-00548-x

Online ISSN 1875-0052
Print ISSN 1229-9197

REGULAR ARTICLE

Polycaprolactone-Based Composite Electrospun Nanofibers as Hybrid Biomaterial Systems Containing Hydroxyl- or Carboxylic Acid-Functionalized Multiwall Carbon Nanotubes

Y. Emre Bulbul[1,2,4] · **Nursel Dilsiz**[2,3]

Received: 14 November 2023 / Revised: 19 March 2024 / Accepted: 28 March 2024
© The Author(s), under exclusive licence to the Korean Fiber Society 2024

Abstract
Composite electrospun nanofibers based on polycaprolactone (PCL) have shown promise in various biomedical applications due to their unique properties. This study investigates the effects of incorporating hydroxyl (–OH)- or carboxylic acid (–COOH)-functionalized multiwall carbon nanotubes (MWCNTs) into PCL matrices. Two types of functionalized additives, MWCNT-OH and MWCNT-COOH, were used at different concentrations (0.06 and 0.12 wt%). Various characterization techniques including FTIR, XRD, AFM, SEM, water contact angle analysis, and tensile strength testing were employed to evaluate changes in nanofiber morphology, crystallinity, surface topography, wettability, and mechanical properties. In addition, in vitro cytotoxicity assays were conducted using HUVECs and L929 fibroblasts over 1-, 3-, and 5-day intervals. This study represents a novel examination of (–OH)- and (–COOH)-functionalized MWCNTs as additives in electrospun PCL biopolymer matrices. The findings indicate that incorporating small amounts of (–OH)- or (–COOH)-functionalized MWCNTs enhances the physicochemical characteristics of PCL nanofibers, making them more suitable for biomedical applications. While both types of functionalized MWCNT additives improved properties compared to pure PCL nanofibers, (–COOH)-functionalized MWCNT-incorporated nanofibers exhibited the most favorable features. In conclusion, this research highlights the potential of tailored PCL-based composite nanofibers containing functionalized MWCNTs as advanced biomaterial systems for biomedical applications, contributing to the development of innovative biomaterials for diverse biomedical contexts.

Keywords Polycaprolactone · Carbon nanotubes · Electrospinning · Composites · Biomedical applications · Nanofibers

1 Introduction

The development of novel biomaterials with tailored properties is imperative to advance the field of tissue engineering and regenerative medicine. Electrospinning, as a versatile and efficient fabrication technique, allows the production of nanofibrous structures resembling the native extracellular matrix. The incorporation of functionalized MWCNTs within PCL electrospun nanofibers presents an opportunity to create hybrid biomaterial systems with synergistic properties. These hybrids can combine the mechanical robustness of MWCNTs with the biocompatibility of PCL, potentially yielding materials suitable for scaffolds, drug delivery carriers, and biomedical devices. Electrospun composite nanofibers or microfibers have recently attracted intensive attention since they can be easily fabricated through the addition of nanoparticles into a polymer solution, thus ending up a composite fiber. Fibrous matrices that have been fabricated by electrospinning display unique characteristics such as high porosity, high surface area/volume ratio, and most importantly, allowing surface and structure designs according to end use. Therefore, they are applied extensively in many areas such as advanced composites, catalysis, sensor technology, water filtration, and biomedical applications [1–6].

✉ Y. Emre Bulbul
yemrebulbul@sdu.edu.tr; emrbulbul@gmail.com

1 Department of Chemistry, Faculty of Engineering and Natural Sciences, Suleyman Demirel University, 32220 Isparta, Turkey

2 Department of Chemical Engineering, Graduate School of Natural and Applied Sciences, Gazi University, 06570 Ankara, Turkey

3 Department of Chemical Engineering, Faculty of Engineering, Gazi University, 06570 Ankara, Turkey

4 Present Address: Department of Chemistry, Engineering and Natural Sciences, Suleyman Demirel University, 32260 Isparta, Turkey

Published online: 20 April 2024

Especially, their promising structural features make them suitable candidates in the biomedical field as a drug carrier, wound dressing, and tissue scaffold [7, 8].

Polycaprolactone (PCL) is a Food and Drug Administration (FDA)-certified, non-toxic, biocompatible, and biodegradable semi-crystalline synthetic polymer commonly used in biomedical applications [3, 9]. However, because of its low hydrophilicity, PCL has low cellular affinity [9]. Furthermore, the weak mechanical features of the PCL electrospun nanofibers due to the porous fibrous structure limit their application [9]. Superior physicochemical features and biocompatibility are of significance to the fabrication of electrospun nanofiber for biomedical applications. Therefore, one approach involves fabricating nanofibers by blending PCL with other materials. The addition of hydrophilic polymers and nanoparticles has been applied to come through the shortcomings of PCL and to improve its performance in applications. For instance, a study by H.H. Kao et al investigated the fabrication of nanofibers from a PCL and PCL/chitosan blend to enhance the cellular response of mesothelial cells [10]. Similarly, *Pinus radiata* bark extracts were loaded onto PCL/gelatin nanofibers to improve their biocompatibility for wound healing applications [8].

The incorporation of multiwall carbon nanotubes (MWCNTs) into a polymer matrix, such as polycaprolactone (PCL), has attracted significant attention from researchers due to its potential applications in biomedical domains [11, 12]. However, challenges such as cytotoxicity, hydrophobic nature, and inadequate dispersion of pristine carbon nanotubes within the polymer matrix have hindered its widespread exploration [13, 14]. To address these challenges, it is crucial to thoroughly investigate factors affecting the suitability of MWCNTs for biomedical applications, including nanotube dimensions (length and diameter), presence of functional groups, structural distinctions (multi-wall versus single wall), and the interaction between carbon nanotubes and target cells or tissues [13, 14]. In addition, it is important to note that material properties can diverge based on the chosen fabrication technique. Given these considerations, our objective was to create fibrous biocomposites via electrospinning, integrating minimal amounts of hydroxyl- and carboxyl-functionalized. The (–OH) and (–COOH) groups were chosen based on their ability to modify the surface properties of MWCNT and PCL nanofibers, as well as their potential to enhance adhesion, growth, and interaction with other materials. The selection of (–OH) and (–COOH) functional groups for functionalized MWCNT and PCL nanofibers is supported by their demonstrated impact on the properties, interactions, and applications of the resulting materials. The literature provides evidence of the crucial role of these functional groups in modifying surface properties, enhancing adhesion and growth, influencing toxicity, determining material applications, and affecting cellular interactions. Moreover, the selection of (–OH) and (–COOH) functional groups for functionalized MWCNTs aligns with previous research in the field of nanofiber composites. For instance, in the context of bone tissue engineering, the use of functional groups, such as (–OH), has been shown to enhance cytocompatibility and osteogenesis in composite nanofibers [15]. This indicates that these functional groups can positively influence the biological properties of the nanofiber composites, making them suitable for biomedical applications.

The effects of two different functionalized additives, specifically MWCNT-OH and MWCNT-COOH, along with different amounts of additives (0.06 and 0.12 wt%), were studied to understand their influence on the properties of the material. This investigation involved employing a variety of methods, such as FTIR, XRD, AFM, SEM, water contact angle analysis, and tensile strength testing, to analyze changes in the material's characteristics. In addition, an in vitro cytotoxicity assay was conducted to assess potential toxicity to HUVECs and L929 fibroblasts over 1-, 3-, and 5-day intervals.

2 Experimental

2.1 Materials

Polycaprolactone pellets with an average molecular weight of 80,000 were procured, along with dimethylformamide (DMF) of ACS reagent grade (≥ 99.8%), tetrahydrofuran (THF) containing 250 ppm of BHT as an inhibitor, also of ACS reagent grade (≥ 99.0%). In addition, dimethyl sulfoxide (DMSO) labeled as PCR reagent, methylthiazolyldiphenyl-tetrazolium bromide (MTT), Dulbecco's modified Eagle's medium with high glucose (DMEM), and phosphate buffer saline tablets (PBS) were all sourced from Sigma Aldrich Co., Ltd., USA, and were utilized as received. We obtained OH-modified and COOH-modified multiwall carbon nanotubes (MWCNTs) with outer diameters ranging from 10 to 20 nm and lengths of 30 μm, boasting a purity level of over 95 wt%. These MWCNTs also featured functional groups, constituting 2–3 wt%. These carbon nanotubes were acquired from Chengdu Organic Chemicals Co. Ltd, specifically from Times Nano.

2.2 Solution Preparations for Electrospinning

The polymer solution containing 15 wt% PCL was prepared in a solvent system containing DMF/THF at a volume ratio of 70:30. To obtain MWCNT-incorporated biocomposite nanofibers, different concentrations of MWCNTs were added to the PCL solution. The concentration of PCL was kept constant to evaluate the influence of MWCNTs on the electrospun biocomposite nanofibers. To ensure the dissolution of

the PCL and proper mixing of MWCNTs, all solutions were stirred overnight with a magnetic stirrer. To remove the air bubbles, the final solutions were ultrasonicated for 2 h before the electrospinning process. The detailed composition of the electrospinning solutions is given in Table 1.

2.3 Electrospinning Process

The 5-mL syringes contained individual solutions and were employed in the electrospinning procedure using Teknotip equipment from Turkey. To achieve a desirable morphology devoid of any bead defects, the following parameters were meticulously optimized: solution flow rates (500 μL h^{-1}), applied voltage (15 kV), and the distance between the grounded collector and the needle tip (17.5 cm). The electrospinning process was conducted under ambient conditions of room temperature and humidity.

2.4 Characterizations of Electrospun Biocomposite Nanofibers

2.4.1 SEM Analysis

Electrospun nanofibers were meticulously positioned onto an SEM grid. Prior to the experiment, each sample underwent a gold-coating process using a Polaron SC 502 sputter coater. The analysis of these samples was conducted using a JEOL JSM 6060 LV model scanning electron microscope, operating at an acceleration voltage of 10 kV. Subsequently, the Digimizer Image Analysis Software (Softpedia) was employed for determining the average fiber diameter from the SEM images. The measurements encompassed 60 randomly selected individual fibers and were presented as the specimens' mean diameter along with the standard deviation.

2.4.2 AFM Analysis

AFM investigations were conducted utilizing the AFM Park Systems instrument (Park XE-100). To capture surface topography images of the specimens, a piezo scanner was employed, covering areas of 20×20 μm^2. These topographical analyses were executed under room temperature conditions, with a scanning rate of 1 Hz, employing the tapping mode.

The surface roughness of individual fibers was evaluated using the upper portions of the topography images, consistent with our previous methodology [16]. Roughness values were derived by randomly selecting 35 fibers for each sample. Figure 1 illustrates the process of calculating surface roughness on the fibers and the resulting roughness profile. All calculations, including topography and surface roughness, were performed using the XEI-7 Image Processing Program software developed by Park Systems Corp.

2.4.3 FTIR Analysis

FTIR spectroscopy was employed to analyze the functional chemical bonds present in the composite nanofibers that were developed. This analysis was conducted using a Nicolet FTIR Spectrometer. A specimen of the composite nanofibers was positioned on the instrument's inspection surface, and the spectra were recorded across a wavelength range spanning from 600 to 4000 cm^{-1}. The acquired spectra were subsequently analyzed using the OMNIC viewer software from Thermo Fisher Scientific.

2.4.4 XRD Analysis

X-ray diffraction (XRD) examinations were conducted using an APD 2000 PRO diffractometer from GNR, USA, to validate the produced composite nanofiber structures. The diffraction patterns were recorded at a temperature of 25 °C, utilizing CuKα radiation within the 2θ range spanning from 5° to 90°. The scanning rate employed for each sample, including those containing pure (–OH)- and (–COOH)-functionalized MWCNT powders, was set at 1° per minute.

2.4.5 Water CA Analysis

The wettability of the specimen was assessed by measuring the water contact angle (CA) through the sessile drop method, employing the Krüss DSA 100 instrument from Germany. A 3.0 mL pure water droplet was meticulously deposited onto the surface of the specimen using a micro syringe. To ensure accuracy, a minimum of four

Table 1 The compositions of the electrospun biocomposite nanofibers

Biocomposite ID	PCL (wt%)	MWCNT-OH (wt. % with respect to polymer amount)	MWCNT-COOH (wt% with respect to polymer amount)
PCL	15	–	–
PCL/0.06 MWCNT-OH	15	0.06	–
PCL/0.12 MWCNT-OH	15	0.12	–
PCL/0.06 MWCNT-COOH	15	–	0.06
PCL/0.12 MWCNT-COOH	15	–	0.12

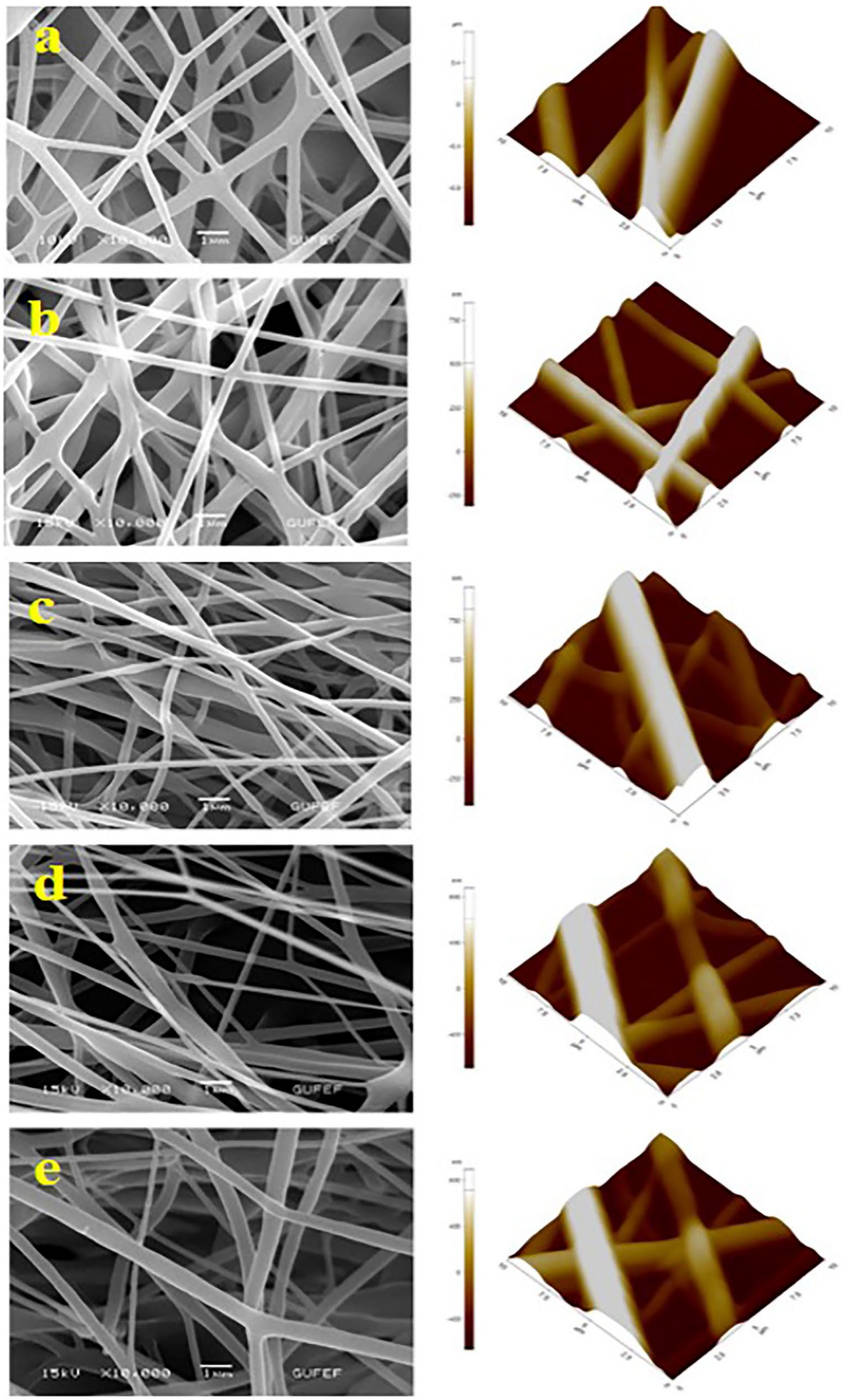


Fig. 1 SEM micrographs of the electrospun biocomposite nanofibers: **a** pure PCL, **b** PCL/0.06 MWCNT-COOH, **c** PCL/0.12 MWCNT-COOH, **d** PCL/0.06 MWCNT-OH, **e** PCL/0.12 MWCNT-OH

measurements were taken from different surface locations for each sample, and the results were subsequently reported as the mean water contact angle of the specimens along with the associated standard deviation.

2.4.6 Tensile Strength Test

The tensile strength of the samples was performed with an AG-I tensile testing machine (Shimadzu, Japan) by applying a 500 N load cell at a crosshead speed of 1 mm/min. All the samples were cut into rectangles with approximate dimensions of 15×20 mm^2 and vertically mounted in between two mechanical gripping units of the tester, leaving approximate 10–30 mm gauge length for mechanical loading. The sample thicknesses were measured with a digital thickness gauge. The thicknesses of the samples ranged from 20 to 30 µm. To calculate tensile strength, the following formula was applied:

$$\sigma = \frac{F}{A}$$

where: σ (N/mm^2) is the tensile strength, F (N) is the force applied to the sample, and A (mm^2) is the cross-sectional area of the sample.

2.4.7 In Vitro Cytotoxicity Evaluation

The cytotoxicity assessment of the electrospun nanofibers was conducted with human HUVECs and L929 fibroblasts. The MTT analysis was carried out using a colorimetric method, as previously documented [17]. In brief, HUVECs and L929 fibroblasts were cultured in DMEM supplemented with 4 Mm L-glutamine, 100 µg/mL streptomycin, 4.5 g/L glucose, 100 µg/mL penicillin, and 10% fetal bovine serum, maintained at 37 °C in a humidified atmosphere containing 5% CO_2.

The specimens were first sterilized with ethylene oxide gas and then placed in 24-well plates. Subsequently, HUVECs were seeded onto the specimens at a density of 5×10^4 cells/cm^2 and placed in a CO_2 incubator. After 1, 3, and 5 days of incubation, the specimens were carefully removed, and MTT solution (prepared in phosphate buffer solution at a concentration of 2.5 mg/mL) was added to each well.

Following a 4-h incubation of MTT at 37 °C, 400 µL of DMSO was added to dissolve the formed crystals. The absorbance values for each well were measured using a microplate reader at a wavelength of 570 nm after gently shaking the plates on an orbital shaker for 5 min. Cell viability values were determined based on the mean absorbance value obtained from at least three wells for each sample.

2.5 Statistical Analysis

All experimental data mentioned in this study were expressed as mean ± standard deviation (SD) for at least $n = 3$. The MTT data were analyzed using standard analysis of Student's t test. The level of significance (p value) was set at < 0.05.

3 Results and Discussion

3.1 Morphological Properties of the Electrospun Nanofibers

The success of the electrospinning process was indicated by the absence of bead formations in the nanofibrous structures, as evidenced in previous studies [22]. Electrospinning was employed to fabricate electrospun biocomposite nanofibers with beadless morphologies, achieved by electrospinning solutions containing varying proportions of hydroxyl (–OH)- and carboxylic acid (–COOH)-functionalized multiwall carbon nanotubes (MWCNTs). The outcomes are depicted in Fig. 1a–e. Figure 1a illustrates the smooth and beadless nanofibers obtained from the pure polycaprolactone (PCL) solution via electrospinning.

In addition, the morphologies of PCL/MWCNT electrospun biocomposite nanofibers reinforced with (–OH)- and (–COOH)-functionalized MWCNTs are presented in Fig. 1b–e. The results indicated that the nanofiber morphology remained unaffected by the introduction of both (–OH)- and (–COOH)-functionalized MWCNTs, showing no bead formation. Nevertheless, a notable reduction in the average fiber diameters was observed upon the integration of both types of functionalized MWCNTs within the fibrous PCL matrix. To quantify this, average fiber diameters were calculated using Digimizer Image Analysis Software based on fifty randomly selected individual fibers per sample [23], with the calculated values presented in Fig. 2.

For pure PCL nanofibers, the average diameter was determined as 368 ± 88 nm. Incorporation of MWCNT-COOH led to a decrease in the average diameters. The average diameters of biocomposite nanofibers containing 0.06 wt% and 0.12 wt% of MWCNT-COOH were calculated as 321 ± 48 nm and 280 ± 61 nm, respectively. Similarly, for biocomposite nanofibers containing 0.06 wt% and 0.12 wt% of MWCNT-OH, average diameters of 328 ± 105 nm and 350 ± 146 nm were obtained. The observed reduction in average diameters with the addition of both MWCNT-COOH and MWCNT-OH suggests a synergistic effect on the nanofiber morphology. Notably, MWCNT-COOH induced a greater reduction in average fiber diameter compared to MWCNT-OH. This difference in impact between the (–OH)- and

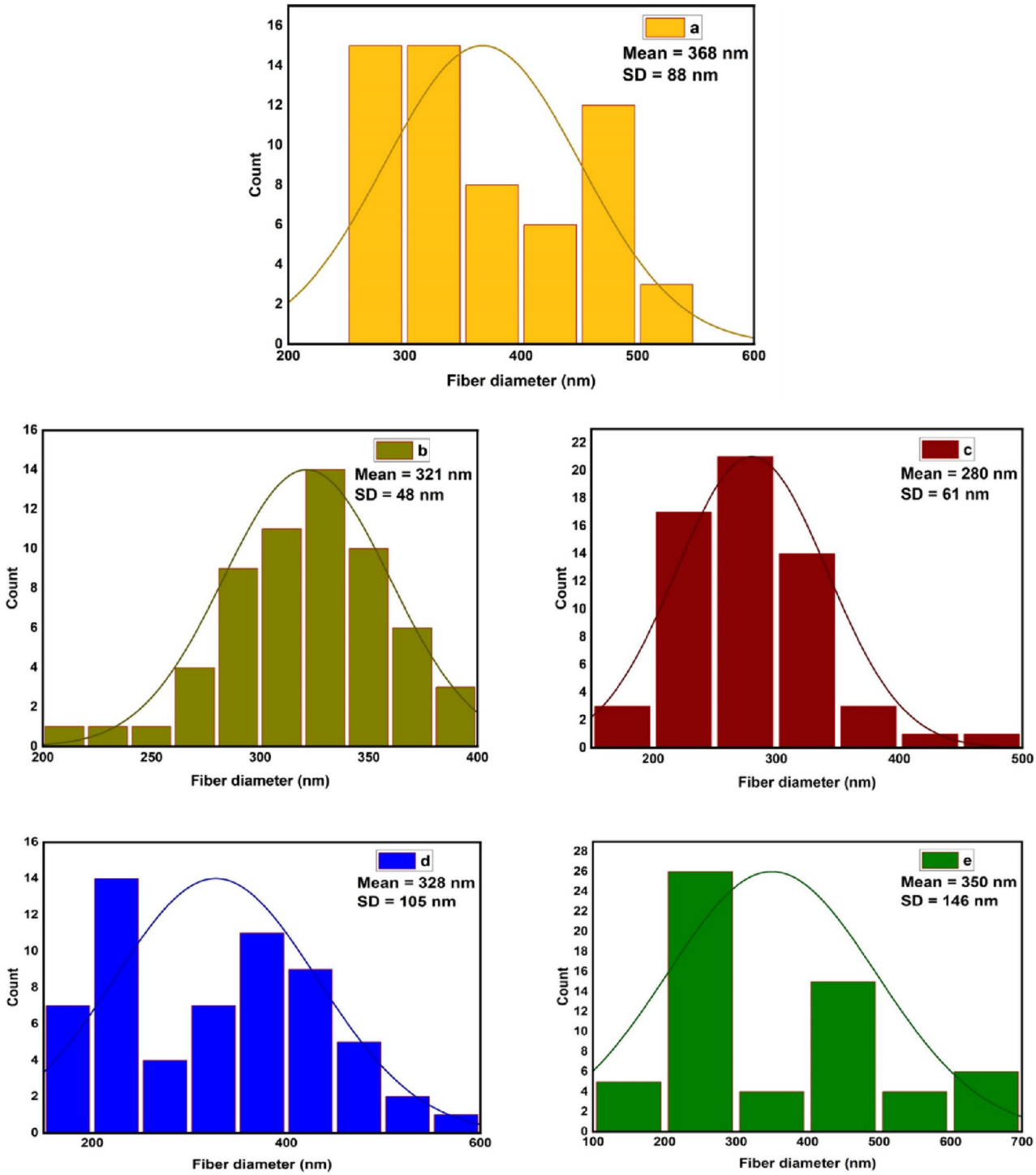


Fig. 2 Average diameter of the electrospun nanofibers: **a** pure PCL, **b** PCL/0.06 MWCNT-COOH, **c** PCL/0.12 MWCNT-COOH, **d** PCL/0.06 MWCNT-OH, **e** PCL/0.12 MWCNT-OH

(–COOH)-functionalized MWCNTs highlights the importance of surface functionalization in influencing the properties of biocomposite nanofibers. The presence of functional groups on the surface of MWCNTs provides sites for the formation of nanoparticles, which can lead to stronger nanotube-polymer interactions and result in a reduction in nanofiber diameter [18, 19]. The improved dispersion and adhesion of functionalized MWCNTs in polymer matrices can also contribute to the reduction in nanofiber diameter [20, 21].

AFM was employed to meticulously characterize the surface properties of the electrospun nanofibers. The three-dimensional AFM topography images of the pristine PCL nanofibers, PCL/MWCNT-OH, and PCL/MWCNT-COOH electrospun biocomposite nanofibers are depicted in Fig. 1a–e. Evidently, the AFM topography images universally exhibited smooth and bead-free surface morphologies across all obtained electrospun nanofibers. These AFM observations were consistent with the outcomes derived from SEM. The AFM results unveiled that the integration of MWCNTs into the PCL matrix significantly influenced the surface roughness of the electrospun biocomposite nanofibers. In particular, the pristine PCL nanofibers demonstrated an average surface roughness of 80 ± 25 nm. Remarkably, with an escalation in the content of MWCNT-OH and MWCNT-COOH in the PCL polymer matrix from 0 wt% to 0.12 wt%, the surface roughness underwent substantial augmentation, elevating to 224 ± 102 nm and 910 ± 295 nm, respectively. Assessing the nanoscale surface morphology of composite materials assumes pronounced significance in predicting material performance-associated characteristics. Notably, in the realm of biomedicine, the interplay between cell and material surface holds direct implications for performance, thereby elevating the importance of comprehending these attributes. The same observations were reported by Cheng et al., who noted that the surface roughness of PLGA/CNT composite films increased proportionally with escalating CNT concentrations [20]. Remarkably, the present study discerned a more pronounced enhancement in surface roughness with MWCNT-COOH compared to MWCNT-OH. This discernment can be attributed to the uniform dispersion of MWCNTs within the PCL fibrous matrix, which fosters heightened specific interactions with the polymer chains, as previously underscored by the works of other researchers.

3.2 Physicochemical and Mechanical Properties of the Electrospun Nanofibers

The FTIR spectra of distinct specimens, including pure PCL nanofibers, PCL/MWCNT-OH, and PCL/MWCNT-COOH biocomposite nanofibers, are depicted in Fig. 3. The pure PCL nanofibers exhibited a characteristic peak at around 1720 cm^{-1}, corresponding to the ester carbonyl stretching [22, 23]. Symmetric C–H stretching and asymmetric CH_2 stretching bands emerged at 2862 cm^{-1} and 2942 cm^{-1}, respectively, in accordance with previous reports [23, 24]. The appearance of a peak at 1745 cm^{-1} could be attributed to C = O stretching, signifying the presence of –OH or –COOH groups. The shifting or increase in peak intensity of the main PCL peaks in the FTIR spectrum of PCL nanofibers from PCL/MWCNT-OH and PCL/MWCNT-COOH nanofibers can be attributed to various factors. When PCL is combined with different materials or functional groups, it can lead to

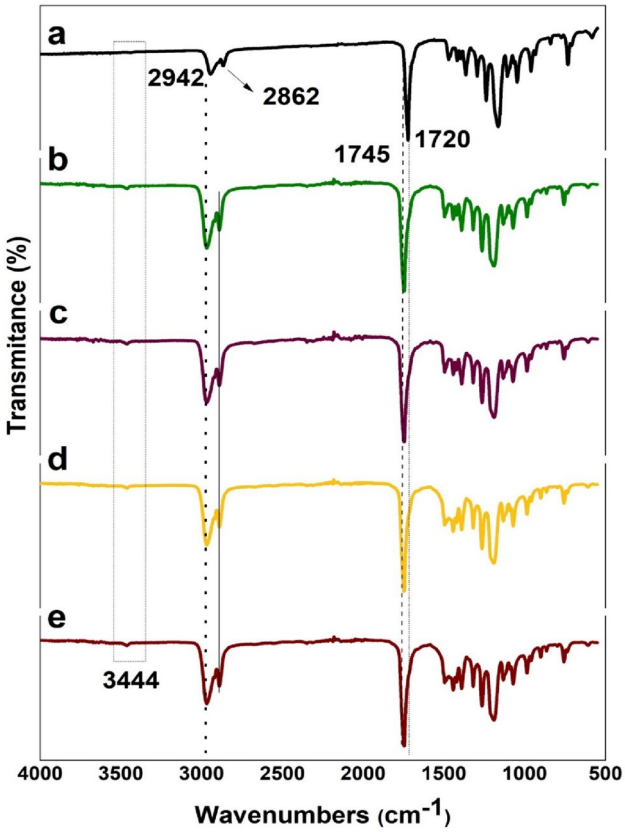


Fig. 3 FTIR spectra of the electrospun biocomposite nanofibers: **a** pure PCL, **b** PCL/0.06 MWCNT-COOH, **c** PCL/0.12 MWCNT-COOH, **d** PCL/0.06 MWCNT-OH, **e** PCL/0.12 MWCNT-OH

changes in the FTIR spectrum due to interactions between the components. In the case of PCL/MWCNT-OH nanofibers, the formation of hydrogen bonds between the hydroxyl group in the polyphenol and the carbonyl group in PCL can cause a slight shift in the characteristic peak of PCL [25]. This interaction between the hydroxyl group and carbonyl group can affect the vibrational modes of the PCL molecule, leading to changes in peak positions in the FTIR spectrum. Similarly, in PCL/MWCNT-COOH nanofibers, the presence of carboxyl groups from the MWCNT-COOH can also influence the FTIR spectrum of PCL. The characteristic peak of PCL due to the ester carbonyl stretching at 1734 cm^{-1} and CH_2 stretching vibrations at 2942 cm^{-1} and 2867 cm^{-1} can be affected by the presence of carboxyl groups [26]. The interaction between the carboxyl groups and the PCL molecule can lead to changes in peak intensities and positions in the FTIR spectrum. Moreover, the relative intensity of the peak of PCL can also increase with the incorporation of certain materials. For instance, in nanofibrous mats containing chitosan/PCL/*Myrtus communis* L. extract, the intensity of the peak slightly increased with an increase in the amount of *Myrtus communis* L. extract [27]. This increase in peak intensity can be attributed to the enhanced interactions

between the components, leading to changes in the FTIR spectrum.

Figure 4 displays the XRD patterns of various materials under examination, including pristine PCL nanofibers, all biocomposite nanofibers, and pure samples of MWCNT-COOH and MWCNT-OH. The graphs reveal prominent diffraction peaks at Bragg angles $2\theta = 21.3°$ and 23.7°, corresponding to the (1 1 0) and (2 0 0) lattice planes of semi-crystalline PCL, respectively [28–30]. Notably, the XRD patterns of PCL/MWCNT-COOH and PCL/MWCNT-OH composites retain the distinctive peaks of pure PCL, indicating that the incorporation of MWCNTs has minimal impact on the crystalline structure of PCL. These findings align with previous studies on polymer/MWCNTs composites [17, 31].

WCA measurements were conducted to assess the wettability characteristics of electrospun biocomposite nanofibers, with results presented in Fig. 5. The water CA value for pristine PCL nanofibers was measured at 133.7° ± 0.8°. Upon the introduction of 0.06 wt% and 0.12 wt% MWCNT-COOH into the PCL matrix, the water CA decreased progressively from 133.7° ± 0.8° to 104° ± 0.3° and 98° ± 0.8°, respectively. Conversely, upon incorporation of 0.06 wt% and 0.12 wt.% MWCNT-OH, the water CAs were measured at 118° ± 1.2° and 101° ± 1.6°, respectively. The hydrophobic nature of pure PCL nanofibers is a well-established characteristic in the literature. PCL nanofibers inherently exhibit hydrophobic properties due to the absence of polar functional groups on their surface [32]. This hydrophobicity is evident in studies where the contact angle measurements of pure PCL nanofibers show high water contact angles, indicating their hydrophobic nature [24, 33, 34]. However, the addition of certain components can alter this property. The findings underscored that water CAs of the electrospun hybrid nanofibers decreased proportionately with augmented MWCNT-COOH and MWCNT-OH concentrations in the PCL matrix. The presence of oxygen-containing groups, such as hydroxyl, carbonyl, and carboxylic groups, on the surface of materials like MWCNTs has been shown to enhance hydrophilicity. Plisko et al. (2022) demonstrated that incorporating oxidized MWCNTs into membranes led to significant hydrophilization of the membrane surface due to the presence of these hydrophilic oxygen-containing groups [35]. This phenomenon was further supported by Sianipar et al. [36], who reported that oxygen-containing groups like –OH and –COOH on MWCNTs protrude onto the fiber surface, reducing water contact angles and increasing surface hydrophilicity [36]. Accordingly, the findings indicate that the incorporation of MWCNTs containing oxygenated groups, specifically the (–COOH) moiety, facilitates the production of more hydrophilic biocomposite nanofibers.

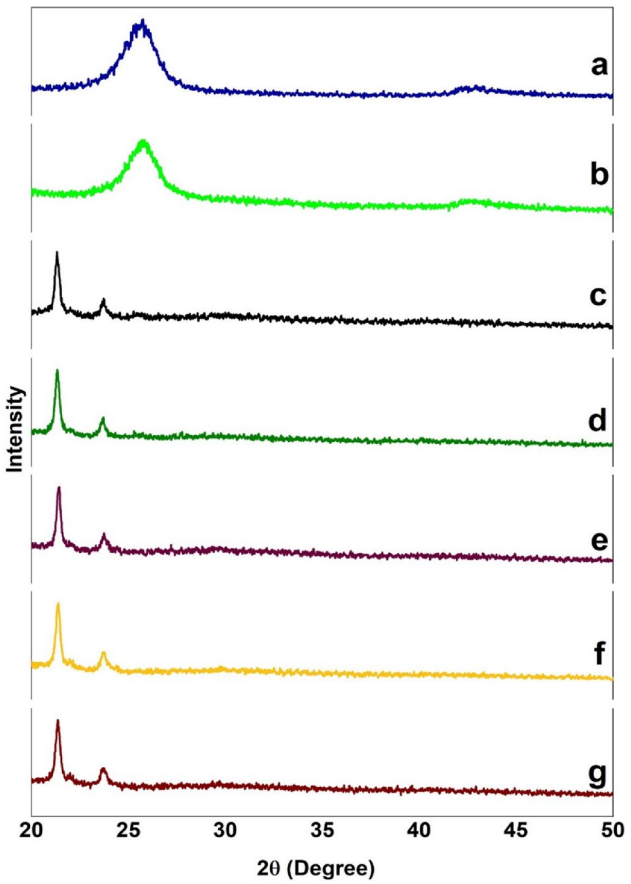


Fig. 4 XRD patterns of the electrospun biocomposite nanofibers: **a** pure MWCNT-OH, **b** pure MWCNT-COOH, **c** pure PCL, **d** PCL/0.06 MWCNT-COOH, **e** PCL/0.12 MWCNT-COOH, **f** PCL/0.06 MWCNT-OH, **g** PCL/0.12 MWCNT-OH

Mechanical characteristics are of paramount importance in biomedical applications due to their relevance across diverse functionalities. Consequently, the mechanical attributes were subjected to meticulous analysis through tensile strength assessment. Both methodologies collectively affirmed that the PCL/MWCNT-OH and PCL/MWCNT-COOH electrospun biocomposite nanofibers exhibited notably elevated mechanical properties when juxtaposed with the unadulterated PCL nanofibers (Fig. 6). The stress–strain profiles of the pristine PCL nanofiber and the electrospun biocomposite counterparts are graphically depicted in Fig. 6. Evidently, the unfilled PCL nanofiber manifested frail mechanical attributes, characterized by a modest tensile strength of 0.9 ± 0.92 MPa. Notably, as depicted in Fig. 5, an escalation in the concentration of both hydroxyl (–OH)- and carboxylic acid (–COOH)-functionalized MWCNTs correlated with an enhancement in the tensile strength of the electrospun nanofibers in comparison to pure PCL. Specifically, the tensile strengths of the electrospun biocomposite nanofibers impregnated with MWCNT-COOH were recorded as 2.08 ± 0.2 MPa and 2.28 ± 0.4 MPa for PCL/0.06 MWCNT-COOH and PCL/0.12 MWCNT-COOH,

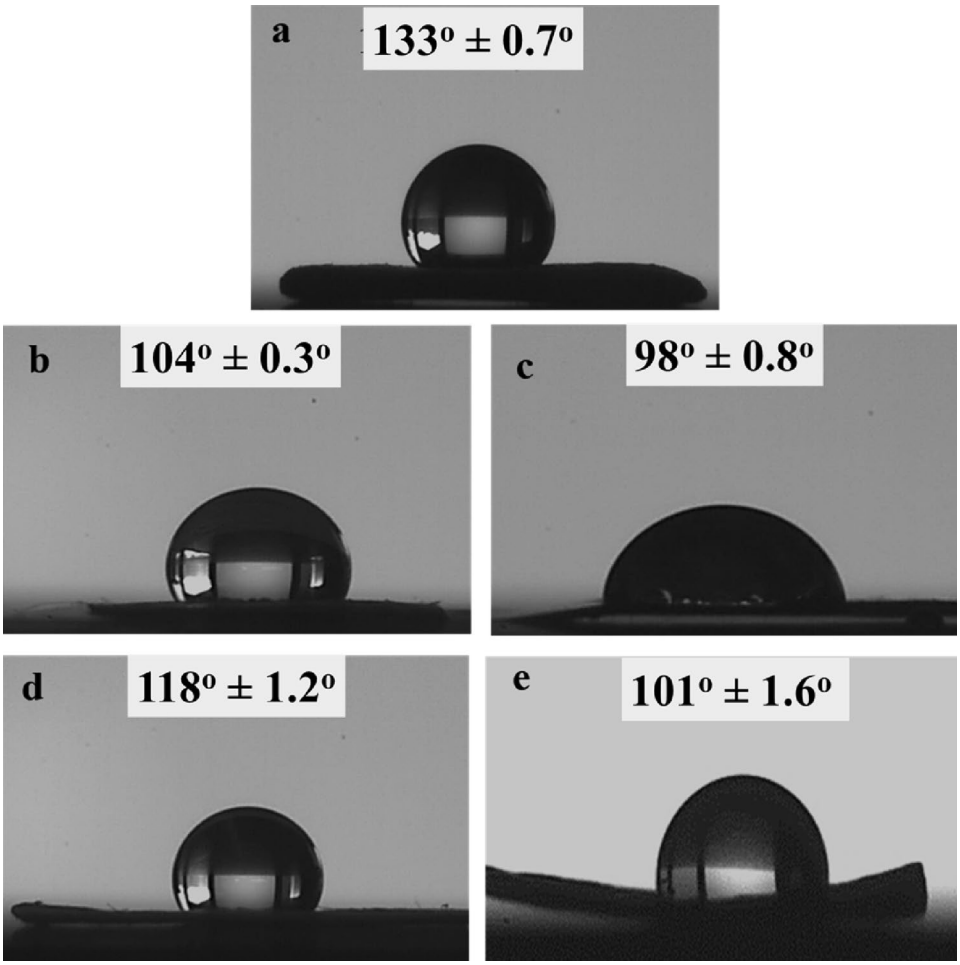


Fig. 5 Water contact angles of the electrospun biocomposite nanofibers: ($n=4$); **a** pure PCL, **b** PCL/0.06 MWCNT-COOH, **c** PCL/0.12 MWCNT-COOH, **d** PCL/0.06 MWCNT-OH, **e** PCL/0.12 MWCNT-OH

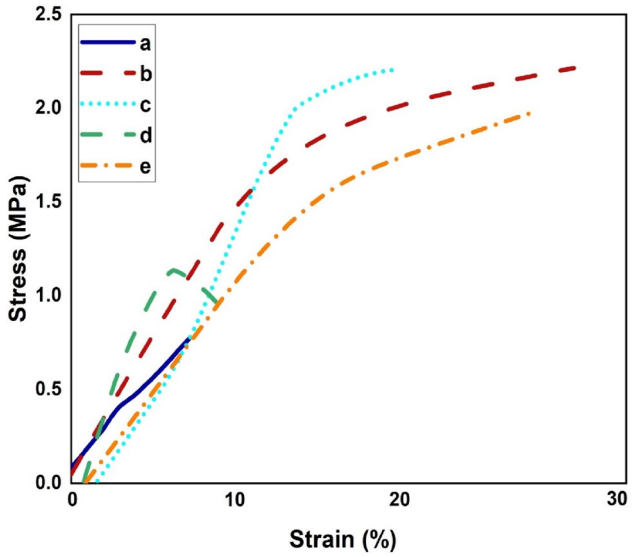


Fig. 6 Tensile strength results of the electrospun biocomposite nanofibers ($n=3$): **a** pure PCL, **b** PCL/0.06 MWCNT-COOH, **c** PCL/0.12 MWCNT-COOH, **d** PCL/0.06 MWCNT-OH, **e** PCL/0.12 MWCNT-OH

respectively. In a parallel vein, the MWCNT-OH-infused electrospun nanofibers exhibited tensile strengths of 1.2 ± 0.25 MPa and 1.9 ± 0.4 MPa for PCL/0.06 MWCNT-OH and PCL/0.12 MWCNT-OH, respectively. These findings collectively underscore the substantial reinforcement in mechanical robustness imparted by the incorporation of MWCNTs, particularly in the form of MWCNT-COOH.

The incorporation of MWCNTs into electrospun nanofibers has been demonstrated to significantly enhance their tensile strength. Various studies have explored different methods of preparing these nanofibers with MWCNTs to achieve improved mechanical properties. For instance, the strength of functionalized MWCNT-reinforced polymer nanocomposites was investigated and the impact of incorporating carboxyl-functionalized MWCNTs into a polymer matrix was highlighted [37]. This study demonstrated the potential for enhancing the mechanical properties of nanocomposites through the addition of MWCNTs.

Moreover, the work by E. Bahmani et al showcased the fabrication of nanofibers for breast cancer treatment by doping MWCNTs into a polymer matrix, emphasizing the cytotoxicity enhancement achieved through this approach

[38]. In addition, Alruwaili et al. studied the reinforcement of biodegradable polymer blends with MWCNTs, focusing on the influence of MWCNT concentration on the tensile properties of the nanocomposites [39]. These studies collectively underscore the versatility of MWCNTs in improving the mechanical performance of polymer nanofibers. In this study, notable advancements in tensile strength were achieved by integrating MWCNT-COOH into the PCL polymer matrix, elevating the value from 0.9 to 2.28 MPa, an increase of approximately 153.3%.

3.3 In Vitro Cytotoxicity Evaluation

The evaluation of cellular response to developed biomaterials is imperative to ensure their biocompatibility for potential biomedical applications. In this regard, two prominent models for cytocompatibility assessment in the realm of biomedical engineering are HUVECs and L929 fibroblast cells. Therefore, the cytotoxicity studies of the fabricated biocomposites were systematically conducted using HUVECs and L929 cells. The MTT assay was employed to determine the cell viability of HUVECs and L929 cells after exposure to the developed biocomposite nanofibers. In addition, the influence of PCL itself was evaluated independently of multiwall carbon nanotubes (MWCNTs) to ascertain the absence of any inherent toxicity unrelated to MWCNTs. Cells were seeded in multiwell plates and were allowed to incubate for 1, 3, and 5 days. As depicted in Fig. 7, the cell viabilities for L929 and HUVEC cells were above 80%, when exposed to the MWCNT-containing hybrid nanofibers. As per the ISO 10993–5 standards, a cell viability exceeding 80% is indicative of non-cytotoxic behavior [40, 41]. Thus, the MTT assay outcomes underscore that the electrospun biocomposite nanofibers synthesized herein exhibited non-cytotoxic behavior toward both HUVEC and L929 cell lines. Remarkably, the PCL/MWCNT-COOH electrospun biocomposite nanofibers showcased an even higher degree of biocompatibility than the PCL/MWCNT-OH counterpart.

Drawing from the relevant references provided, it becomes apparent that MWCNTs, when appropriately functionalized, can exhibit non-toxic effects on cell viability and proliferation [42–44]. For instance, studies have demonstrated that functionalization with carboxyl or amino groups can effectively mitigate the toxic effects of pristine MWCNTs in macrophages [42]. Moreover, investigations indicate that functionalized MWCNTs do not pose toxicity concerns toward PC-12 neuronal cells [43]. These findings underscore the significance of surface modification in augmenting the biocompatibility of MWCNTs. On the contrary, some investigations have reported cytotoxicity associated with elevated concentrations of MWCNTs [45, 46]. For instance, studies have shown that the extract of hydrogel loaded with MWCNTs led to a significant decrease in the viability of cancer cells, while noncancerous cells exhibited higher viability [46]. In addition, non-functionalized MWCNTs were observed to induce apoptosis in human cells [45]. These findings underscore the importance of carefully considering MWCNT concentrations to mitigate cytotoxic effects. Moreover, the cytocompatibility of MWCNTs can vary depending on their functionalization and dispersion state [44]. Agglomerates of MWCNTs were found to be less toxic than dispersed forms, as larger agglomerates reduce the available surface for interaction with cells [44]. In addition, the juxtaposition of diols with MWCNTs was shown to decrease the toxicity of MWCNTs due to enhanced dispersibility [47].

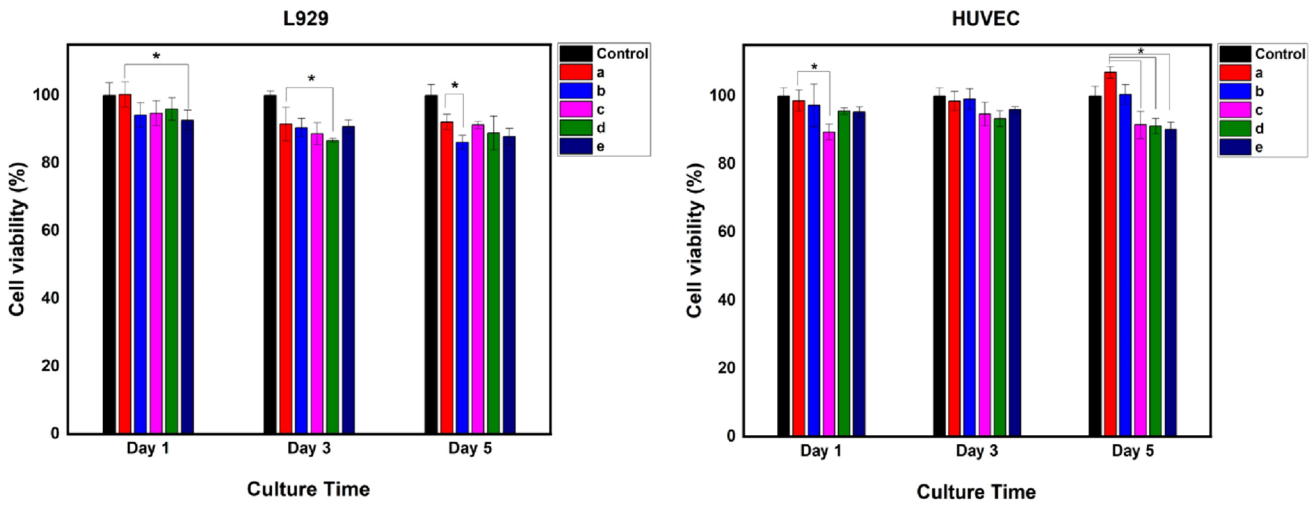


Fig. 7 Cell viability of the electrospun biocomposite nanofibers for the HUVECs and L929: **a** pure PCL, **b** PCL/0.06 MWCNT-COOH, **c** PCL/0.12 MWCNT-COOH, **d** PCL/0.06 MWCNT-OH, **e** PCL/0.12 MWCNT-OH. Data are expressed as mean ± standard deviation (SD), $n = 3$, $^*p < 0.05$ vs. PCL nanofibers group

In conclusion, the biocompatibility of MWCNTs is influenced by various factors such as functionalization, concentration, and dispersion state. Proper functionalization of MWCNTs can enhance their biocompatibility, while high concentrations and non-functionalized forms may lead to cytotoxic effects. Understanding these factors is crucial for the safe and effective utilization of MWCNTs across various applications.

4 Conclusion

In the current study, biocompatible electrospun nanofibers were successfully prepared using the electrospinning method, incorporating functionalized MWCNTs into the PCL matrix. The outcomes of this investigation have shed light on the distinct behavior of functionalized MWCNTs when introduced into PCL nanofibers. The morphological analysis revealed that both PCL/MWCNT-OH and PCL/MWCNT-COOH electrospun biocomposite nanofibers maintained comparable morphologies to pure PCL, with variations in the average fiber diameter corresponding to the concentration of incorporated MWCNTs. Notably, the tensile strength of the composite nanofibers experienced remarkable enhancements when the highest concentrations of MWCNT-OH and MWCNT-COOH were introduced, showing increases of 111% and 153%, respectively, from 0.9 MPa to 2.28 MPa and 1.9 MPa. The water contact angle (CA) values, which were $133.7° \pm 0.8°$ for pure PCL, decreased to $98° \pm 0.8°$ and $101° \pm 1.6°$ with the highest additions of MWCNT-OH and MWCNT-COOH, respectively, indicating increased hydrophilicity. When collectively evaluated, the MWCNT-COOH-incorporated nanofibers exhibited superior mechanical strength, cytocompatibility, surface roughness, and hydrophilicity compared to MWCNT-OH counterparts within the PCL fibrous matrix.

Supplementary Information The online version contains supplementary material available at https://doi.org/10.1007/s12221-024-00548-x.

Acknowledgements This work was funded by the Gazi University Scientific Research Projects Unit Grant number: 06/2020-07.

Funding Open access funding provided by the Scientific and Technological Research Council of Türkiye (TÜBİTAK).

Data availability The raw data required to reproduce these findings are available from the corresponding author upon request.

Declarations

Conflict of Interest The authors declare that they have no conflicts of interest.

References

1. R. Fekrazad, F. Tondnevis, M.M. Abolhasani, In-vitro evaluation of novel polycaprolactone/chitosan/carbon nano tube scaffold for tissue regeneration. J Biomed Phys Eng (2022). https://doi.org/10.31661/jbpe.v0i0.1188
2. H. Li, D. He, X. Xiao et al., Nitrogen-doped multiwalled carbon nanotubes enhance bone remodeling through immunomodulatory functions. ACS Appl. Mater. Interfaces (2021). https://doi.org/10.1021/acsami.1c05437
3. M. Khandaker, H. Progri, D.T. Arasu et al., Use of polycaprolactone electrospun nanofiber mesh in a face mask. Materials (Basel) (2021). https://doi.org/10.3390/ma14154272
4. R. Zhang, X. Li, Y. Liu et al., Acceleration of bone regeneration in critical-size defect using bmp-9-loaded nha/coli/mwcnts scaffolds seeded with bone marrow mesenchymal stem cells. Biomed. Res. Int. (2019). https://doi.org/10.1155/2019/7343957
5. G. Kazemzadeh, N. Jirofti, D. Mohebbi-Kalhori et al., Pathological examination of blended and co-electrospinning hybrid polycaprolactone/polyurethane nanofibers for soft tissue engineering applications. J. Ind. Text. (2022). https://doi.org/10.1177/15280837221074070
6. S. Mirzaeei, M. Mansurian, K. Asare-Addo, A. Nokhodchi, Metronidazole-and amoxicillin-loaded plga and pcl nanofibers as potential drug delivery systems for the treatment of periodontitis: in vitro and in vivo evaluations. Biomedicines (2021). https://doi.org/10.3390/biomedicines9080975
7. E. Sadeghi, S.M. Zebarjad, F. Khademi, E. Bagherzadeh, Enhancing structural strength and improving cell survival through polycaprolactone/(gelatin/hydroxyapatite) core-shell nanofibers for tissue engineering. Polym. Compos. (2022). https://doi.org/10.1002/pc.26819
8. J. Borges-Vilches, I. Unalan, K. Fernández, A.R. Boccaccini, Fabrication of biocompatible electrospun poly(ε-caprolactone)/gelatin nanofibers loaded with *Pinus radiata* bark extracts for wound healing applications. Polymers (Basel) (2022). https://doi.org/10.3390/polym14122331
9. Y. Snyder, S. Jana, Fibrin gel enhanced trilayer structure in cell-cultured constructs. Biotechnol. Bioeng. (2023). https://doi.org/10.1002/bit.28371
10. H.H. Kao, C.Y. Kuo, D. Tagadur Govindaraju et al., Polycaprolactone/chitosan composite nanofiber membrane as a preferred scaffold for the culture of mesothelial cells and the repair of damaged mesothelium. Int. J. Mol. Sci. (2022). https://doi.org/10.3390/ijms23179517
11. K. Lisik, A. Krokosz, Application of carbon nanoparticles in oncology and regenerative medicine. Int. J. Mol. Sci. **22**, 8341 (2021)
12. K. Ashtari, H. Nazari, H. Ko et al., Electrically conductive nanomaterials for cardiac tissue engineering. Adv. Drug Deliv. Rev. **144**, 162–179 (2019)
13. B. Huang, Carbon nanotubes and their polymeric composites: the applications in tissue engineering. Biomanuf Rev (2020). https://doi.org/10.1007/s40898-020-00009-x
14. L.A. Chavez, J.E. Regis, L.C. Delfin et al., Electrical and mechanical tuning of 3D printed photopolymer–MWCNT nanocomposites through in situ dispersion. J. Appl. Polym. Sci. (2019). https://doi.org/10.1002/app.47600
15. X. Gao, J. Song, P. Ji et al., Polydopamine-templated hydroxyapatite reinforced polycaprolactone composite nanofibers with enhanced cytocompatibility and osteogenesis for bone tissue engineering. ACS Appl. Mater. Interfaces (2016). https://doi.org/10.1021/acsami.5b12413
16. Y.E. Bulbul, T. Uzunoglu, N. Dilsiz et al., Investigation of nanomechanical and morphological properties of silane-modified

halloysite clay nanotubes reinforced polycaprolactone biocomposite nanofibers by atomic force microscopy. Polym. Test. (2020). https://doi.org/10.1016/j.polymertesting.2020.106877
17. Y.E. Bulbul, M. Eskitoros-Togay, F. Demirtas-Korkmaz, N. Dilsiz, Multi-walled carbon nanotube-incorporating electrospun composite fibrous mats for controlled drug release profile. Int. J. Pharm. (2019). https://doi.org/10.1016/j.ijpharm.2019.118513
18. G.M. Neelgund, A. Oki, Deposition of silver nanoparticles on dendrimer functionalized multiwalled carbon nanotubes: synthesis, characterization and antimicrobial activity. J. Nanosci. Nanotechnol. (2011). https://doi.org/10.1166/jnn.2011.3756
19. N.G. Sahoo, H.K.F. Cheng, Y. Pan et al., Strengthening of liquid crystalline polymer by functionalized carbon nanotubes through interfacial interaction and homogeneous dispersion. Polym. Adv. Technol. (2011). https://doi.org/10.1002/pat.1704
20. M. Amirian, J. Sui, A.N. Chakoli, W. Cai, Properties and degradation behavior of surface functionalized MWCNT/poly(L-lactide-co-ε-caprolactone) biodegradable nanocomposites. J. Appl. Polym. Sci. (2011). https://doi.org/10.1002/app.34317
21. Q. Zehua, W. Guojian, A comparative study on the properties of the different amino-functionalized multiwall carbon nanotubes reinforced epoxy resin composites. J. Appl. Polym. Sci. (2012). https://doi.org/10.1002/app.35105
22. A. Ujčić, M. Sobótka, M. Šlouf et al., Structure-property relationships in PCL porous scaffolds obtained by means of the TIPS and TIPS-PL methods. Polym. Test. (2023). https://doi.org/10.1016/j.polymertesting.2022.107906
23. M. Kök, M.E. Pekdemir, E. Özen Öner et al., MWCNT nanocomposite films prepared using different ratios of PVC/PCL: combined FT-IR/DFT, thermal and shape memory properties. J. Mol. Struct. (2023). https://doi.org/10.1016/j.molstruc.2023.134989
24. ŞM. Eskitoros-Togay, Y.E. Bulbul, S. Tort et al., Fabrication of doxycycline-loaded electrospun PCL/PEO membranes for a potential drug delivery system. Int. J. Pharm. **565**, 83–94 (2019). https://doi.org/10.1016/j.ijpharm.2019.04.073
25. Y. Wang, X. Wang, D. Zhou et al., Preparation and characterization of polycaprolactone (PCL) antimicrobial wound dressing loaded with pomegranate peel extract. ACS Omega (2023). https://doi.org/10.1021/acsomega.2c08180
26. K.O.I. Altan, Dibenzo-18-crown-6/polycaprolactone composite nanofibers for selective adsorption of cations. Uludağ Univ J Fac Eng (2023). https://doi.org/10.17482/uumfd.1222084
27. T. Modiri-Delshad, A. Ramazani, M. Khoobi et al., Fabrication of chitosan/polycaprolactone/*Myrtus communis* L. extract nanofibrous mats with enhanced antibacterial activities. Polym. Polym. Compos. (2023). https://doi.org/10.1177/09673911231151506
28. H. Chen, Y. Shi, L. Sun, S. Ni, Electrospun composite nanofibers with all-trans retinoic acid and MWCNTs-OH against cancer stem cells. Life Sci. (2020). https://doi.org/10.1016/j.lfs.2020.118152
29. L. Pan, X. Pei, R. He et al., Multiwall carbon nanotubes/polycaprolactone composites for bone tissue engineering application. Colloids Surfaces B Biointerfaces **93**, 226–234 (2012). https://doi.org/10.1016/j.colsurfb.2012.01.011
30. M. Eskitoros-Togay, Y.E. Bulbul, N. Çanga Oymak, N. Dilsiz, Development of poly(Ɛ-caprolactone)-based composite packaging films incorporated nanofillers for enhanced strawberry quality. J. Appl. Polym. Sci. (2023). https://doi.org/10.1002/app.54611
31. S.F. Wang, L. Shen, Z.W. De, Y.J. Tong, Preparation and mechanical properties of chitosan/carbon nanotubes composites. Biomacromol (2005). https://doi.org/10.1021/bm050378v
32. S. Homaeigohar, A.R. Boccaccini, Nature-derived and synthetic additives to poly(ε-caprolactone) nanofibrous systems for biomedicine; an updated overview. Front. Chem. **9**, 809676 (2022)
33. N. Hamdan, W.K.W.A. Khodir, S.A. Hamid et al., PCL/gelatin/graphene oxide electrospun nanofibers: effect of surface functionalization on in vitro and antibacterial response. Nanomaterials (2023). https://doi.org/10.3390/nano13030488
34. W. Wang, Y. Wang, W. Zhao, C. Zhao, A straightforward approach towards antibacterial and anti-inflammatory multifunctional nanofiber membranes with sustained drug release profiles. Macromol. Biosci. (2022). https://doi.org/10.1002/mabi.202200150
35. T.V. Plisko, K.S. Burts, A.V. Bildyukevich, Development of high flux nanocomposite polyphenylsulfone/oxidized multiwalled carbon nanotubes membranes for ultrafiltration using the systems with critical solution temperatures. Membranes (Basel) (2022). https://doi.org/10.3390/membranes12080724
36. Sianipar M, Kim SH, Khoiruddin, et al (2017) Functionalized carbon nanotube (CNT) membrane: Progress and challenges. RSC Adv 7:. https://doi.org/10.1039/c7ra08570b
37. V. Patel, U. Joshi, A. Joshi et al., Strength evaluation of functionalized MWCNT-reinforced polymer nanocomposites synthesized using a 3D mixing approach. Materials (Basel) (2022). https://doi.org/10.3390/ma15207263
38. E. Bahmani, B.F. Dizaji, S. Talaei et al., Fabrication of poly(ϵ-caprolactone)/paclitaxel (core)/chitosan/zein/multi-walled carbon nanotubes/doxorubicin (shell) nanofibers against MCF-7 breast cancer. Polym. Adv. Technol. (2023). https://doi.org/10.1002/pat.5931
39. B.M. Alruwaili, U. Saeed, I. Ahmad et al., Development of multiwalled carbon nanotube-reinforced biodegradable polylactic acid/polybutylene succinate blend membrane. Membranes (Basel) (2021). https://doi.org/10.3390/membranes11100760
40. ISO/International Organization for Standardization, ISO 10993–5 Biological evaluation of medical devices—part 5: tests for cytotoxicity: in vitro methods. Int Organ Stand (2009). https://doi.org/10.1016/j.transproceed.2009.12.077
41. G. Huerta-Ángeles, K. Knotková, P. Knotek et al., Aligned nanofibres made of poly(3-hydroxybutyrate) grafted to hyaluronan for potential healthcare applications. J. Mater. Sci. Mater. Med. (2018). https://doi.org/10.1007/s10856-018-6045-5
42. A. Haroun, Z. Gospodinova, N. Krasteva, Amino acid functionalization of multi-walled carbon nanotubes for enhanced apatite formation and biocompatibility. Nano Biomed Eng (2021). https://doi.org/10.5101/nbe.v13i4.p380-393
43. P.P. Komane, P. Kumar, Y.E. Choonara, V. Pillay, Functionalized, vertically super-aligned multiwalled carbon nanotubes for potential biomedical applications. Int. J. Mol. Sci. (2020). https://doi.org/10.3390/ijms21072276
44. I.F. Silva, L.F. Papa, P.G. Carneiro et al., Primary culture macrophages from fish as potential experimental model in toxicity studies with multiwalled carbon nanotubes. Acta Sci Biol Sci (2021). https://doi.org/10.4025/actascibiolsci.v43i1.52612
45. F. Kabirian, P. Baatsen, M. Smet et al., Carbon nanotubes as a nitric oxide nano-reservoir improved the controlled release profile in 3D printed biodegradable vascular grafts. Sci. Rep. (2023). https://doi.org/10.1038/s41598-023-31619-3
46. F.K. García Verdugo, M.B. Salazar Salas, L. Hanaiy Chan Chan et al., Nanocomposite hydrogels based on poly(vinyl alcohol) and carbon nanotubes for NIR-light triggered drug delivery. ACS Omega **9**, 11860–11869 (2024). https://doi.org/10.1021/acsomega.3c09609
47. K. Brzóska, S. Boncel, M. Dzida et al., Bio-based nanofluids of extraordinary stability and enhanced thermal conductivity as sustainable green heat transfer media. ACS Sustain Chem Eng (2021). https://doi.org/10.1021/acssuschemeng.1c01944